The frequency-domain infrared spectrum of ammonia encodes changes in molecular dynamics caused by a DC electric field

Youngwook Park[a], Hani Kang[a], Robert W. Field[b,1], and Heon Kang[a,1]

[a]Department of Chemistry, Seoul National University, 08826 Seoul, Republic of Korea; and [b]Department of Chemistry, Massachusetts Institute of Technology, Cambridge, MA 02139

Ammonia is special. It is nonplanar, yet in $v = 1$ of the umbrella mode (ν_2) its inversion motion is faster than $J = 0 \leftrightarrow 1$ rotation. Does the simplicity of the Chemist's concept of an electric dipole moment survive the competition between rotation, inversion, and a strong external electric field? NH_3 is a favorite pedagogical example of tunneling in a symmetric double-minimum potential. Tunneling is a dynamical concept, yet the quantitative characteristics of tunneling are expressed in a static, eigenstate-resolved spectrum. The inverting-umbrella tunneling motion in ammonia is both large amplitude and profoundly affected by an external electric field. We report how a uniquely strong (up to 10^8 V/m) direct current (DC) electric field causes a richly detailed sequence of reversible changes in the frequency-domain infrared spectrum (the $v = 0 \rightarrow 1$ transition in the ν_2 umbrella mode) of ammonia, freely rotating in a 10 K Ar matrix. Although the spectrum is static, encoded in it is the complete inter- and intramolecular picture of tunneling dynamics.

infrared spectroscopy | electric field | orientation | inversion | tunneling

Ammonia, a classic example of a symmetric-top molecule, rotates nearly freely inside a solid argon matrix. Only the lowest-energy rotational levels are significantly populated at cryogenic matrix temperature (1–5). Ammonia is fluxional with respect to inversion, with the ν_2 (umbrella mode) infrared fundamental band displaying features that encode the dynamics of inversion by tunneling through a barrier in a symmetric double-minimum potential (1). For $v = 0$, $J = 0 \leftrightarrow 1$ rotation ($2B = 19$ cm^{-1}) is "faster" than inversion (0.8 cm^{-1}) but for $v = 1$, inversion (24 cm^{-1}) is slightly faster than rotation. We apply a direct current (DC) electric field to ammonia molecules with a strength up to 2×10^8 V/m, 2 orders of magnitude stronger than that applied in gas-phase Stark-effect experiments (6, 7) and comparable to that in frozen molecular-film experiments (8). The infrared Stark spectrum of ammonia reveals a sequence of inter- and intramolecular effects: 1) generation of a permanent electric dipole moment along the 3-fold molecular frame symmetry axis (denoted by c) via field-induced mixing of the inversion states, 2) disappearance of the rotational structure accompanied by orientation of molecules with their c axis near-parallel to the laboratory frame field direction (denoted by Z), and 3) systematic changes in the potential energy surface (PES), transition selection rules, intensities, and Stark-tuned transition frequencies. The spectra reflect electric-field-induced changes in the vibrational and rotational PESs. These changes reveal a reduction and, ultimately, a quenching of the inversion dynamics. The DC Stark spectrum illustrates the effects of a strong external electric field on large-amplitude tunneling dynamics in a manner complementary to that observed in focused-laser, ultrafast, "direct-dynamics" experiments.

Results and Discussion

We apply a DC electric field to ammonia molecules isolated in a solid Ar matrix at 10 K by using the ice film nanocapacitor method (9). The spectrum is obtained by reflection-absorption infrared spectroscopy (RAIRS), with the incident light linearly polarized along the direction of the applied field (Z axis). Fig. 1C shows the RAIR spectrum of matrix-isolated NH_3 in the ν_2 (umbrella mode) region and its evolution with increasing field strength. In the zero-field spectrum, the peak at about 975 cm^{-1} corresponds to the $R(0_0^-)$ rovibrational transition ($[v = 0, J = 0, K = 0, -$ inversion symmetry$] \rightarrow [v = 1, J = 1, K = 0, +$ inversion symmetry$]$) of the ν_2 vibrational fundamental band (1). The combination of low temperature, rotation–vibration transition selection rules, and nuclear permutation symmetry reduce the ν_2 band to only 1 transition with significant intensity (*SI Appendix*, section A). Features due to ammonia aggregates (dimer, trimer, etc.) appear at higher frequencies (>990 cm^{-1}) (1, 10) and can be distinguished from the monomer peak by examining their intensity variation with respect to the change in the Ar:NH_3 ratio (*SI Appendix*, Fig. S1). The external field induces drastic changes in the frequency, intensity, and shape of the NH_3 ν_2 band. The $R(0_0^-)$ peak becomes slightly redshifted (to 972 cm^{-1}) and a new peak (963 cm^{-1}) appears at field strength >1.3 × 10^7 V/m. These 2 peaks tune closer to each other as the field increases and eventually merge into a single feature above 4.7 × 10^7 V/m. The merged peak shifts continuously to the blue and increases in intensity as the field increases. These changes are reversible with respect to an increase or decrease of electric-field strength.

Significance

Our experiment captures the detailed sequence of molecular processes that occur when a uniquely strong (∼10^8 V/m) direct current (DC) electric field is imposed on ammonia molecules isolated in a solid Ar matrix. Electric fields are of singular importance in chemistry, materials science, and molecular biology. Intermolecular interactions, resulting in rearrangements of electrons and nuclei, are driven by strong electric fields. The detailed responses of molecules to external electric fields of interatomic strength are incompletely understood, because techniques for applying such strong DC electric fields and observing the molecular responses to these fields do not yet exist. Ammonia, with its extreme amplitude intramolecular dynamics and extreme sensitivity to electric fields, is an ideal subject for study by DC-infrared 2-dimensional spectroscopy.
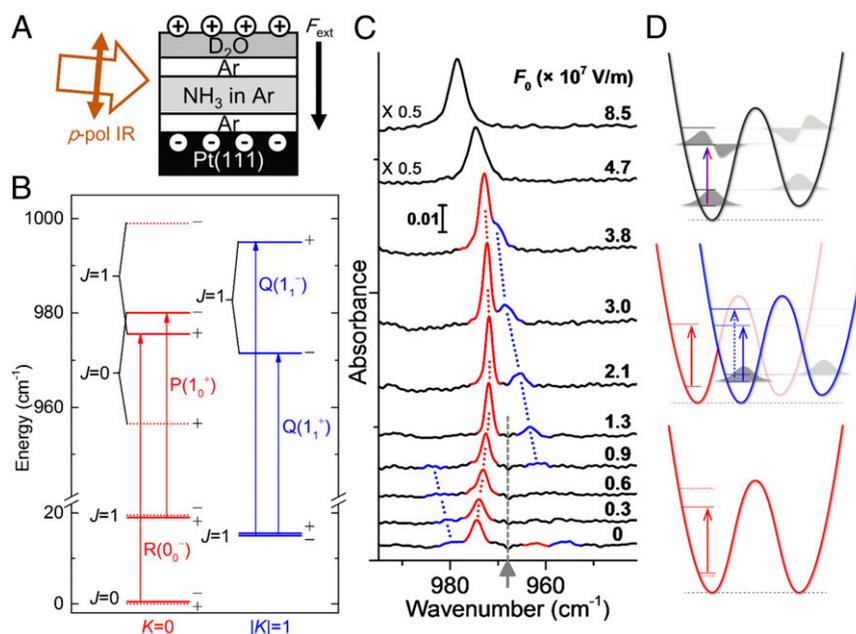

Fig. 1. Vibrational Stark spectroscopy of NH_3 isolated in an Ar matrix. (*A*) The experimental scheme. (*B*) Inversion–rotation–vibration energy levels and transitions of NH_3 at zero field. Below the break in the ordinate is the ground state, $v = 0$, while above is the first excited state of the umbrella vibration, $v = 1$. Energy levels marked with red and blue horizontal lines are those of $K = 0$ and $|K| = 1$, respectively. Dotted horizontal lines indicate the energy levels that are absent due to nuclear permutation symmetry requirements. "+" and "−" signs to the right of the energy levels are the inversion state parity. (*C*) RAIR spectra of the ν_2 umbrella vibration of matrix-isolated NH_3, measured as a function of the strength of applied electric field. The field strength in this figure denotes that of the macroscopic field (F_0) determined directly from the film-voltage measurements (*Methods*). The $v = 0 \rightarrow 1$ vibrational band origin (968 cm^{-1}) is indicated by the upward-pointing gray arrow. In the spectra, transitions occurring between $K = 0$ rotational levels are shown in red, while transitions between $|K| = 1$ states are shown in blue. The evolution of peaks caused by the external field is depicted by dotted red and blue connecting lines. (*D*) Schematic drawings of the double-well potential, energy states, and allowed transitions at different stages of Stark shifts and mixings. Likewise, the red and blue color-coding indicates features that belong to $K = 0$ and $|K| = 1$, respectively. (*Bottom*) A symmetric double-minimum potential at zero field. The transition shown is $R(0_0^-)$, which is prominent at zero field. (*Middle*) The slightly "tilted" asymmetric double-well potential in the intermediate-field region. Energy levels and expected transitions are shown for $K = 0$ (red) and $|K| = 1$ (blue). The red and blue potential curves are identical, but shifted horizontally for clarity. Two strong transitions observed in the intermediate-field region are marked with 2 solid arrows. The dotted blue arrow is an originally allowed transition at zero field but that becomes a forbidden transition as the field strength increases. (*Top*) Strongly asymmetric double-minimum potential in the high-field region. Transitions are localized in the deeper well of the potential and the 2 transitions coincide in energy.

The intensity increase of the ν_2 peak at higher field indicates that the ammonia molecules become dipole-oriented (c axis) along the direction of the field (Z axis). The DC electric field is collinear (Z axis) with the linear polarization axis of the infrared beam (Fig. 1*A*) (11). Thus, the molecular-frame ν_2 band transition moment becomes parallel to the laboratory-frame infrared polarization axis. The evolution of the rotation–vibration spectrum caused by field-induced molecular orientation has been well studied for linear polar molecules in the gas phase (6, 7) and in Ar matrices (12). Those studies have shown that, when the static and radiation fields are collinear, the rotational features in the spectrum gradually disappear and a peak at the vibrational band origin (the location of the rigorously forbidden $[v = 0, J = 0] \rightarrow [v = 1, J = 0]$ transition) becomes dominant when the field-induced molecular orientation (6, 7, 12) is maximized. Symmetric-top rigid rotors show a similar behavior, with slight differences in quantum number dependence (13, 14). The external field mixes the symmetric and antisymmetric inversion states of ammonia, thereby generating a permanent electric dipole moment of the molecule along its c axis. This dipole moment is electrostatically stabilized by becoming oriented parallel to the external field. We will show shortly that the shift and strengthening of the $R(0_0^-)$ peak (red) and the emergence of a new peak (blue) in Fig. 1*C* are consistent with vibrational band-origin transitions of field-oriented molecules.

The increase of the ν_2 band intensity approaches a saturation point at field strength beyond the range displayed in Fig. 1*C* (>1×10^8 V/m) (*SI Appendix*, Fig. S2). This indicates that the orientation of molecules by the field approaches perfection asymptotically. At the same time, the peak shows a blueshift that is linearly dependent on the field strength, which is a manifestation of the expected vibrational Stark shift of the ν_2 frequency of spatially oriented molecules (11) (*SI Appendix*, Fig. S3).

To explain the field-driven spectral changes in the intermediate field region (<5×10^7 V/m), namely the evolution of the $R(0_0^-)$ peak, the appearance of a new peak near 963 cm^{-1}, and the merging of these 2 peaks, we discuss how an external electrostatic field is expected to modify the inversion-rotation-vibration energy levels of NH_3. We note that at low matrix temperature, the only significantly populated rotational states are those with small ($J < 2$ and $|K| < 2$) quantum numbers. Also, under the influence of the external electric field, K remains a good quantum number, indicating that neither electric-dipole-allowed transitions nor field-induced interactions (Stark mixing) occur between states with different K values. Therefore, the field-induced changes can be discussed separately for the $K = 0$ and $|K| = 1$ states.

For $|K| = 1$ states, the $Q(1_1^+)$ and $Q(1_1^-)$ ([$v = 0, J = 1, |K| = 1, \pm$] $\rightarrow$ [$v = 1, J = 1, |K| = 1, \mp$]) transitions at zero field are expected to be located, respectively, at 956 and 980 cm^{-1} (Fig. 1*B*) (1). Transitions within $|K|=1$ are colored blue in the spectra and energy diagrams in Fig. 1. In the zero-field spectrum shown in Fig. 1*C*, the 2 blue peaks correspond to $Q(1_1^+)$ and $Q(1_1^-)$ transitions. They are very weak due to the smaller thermal population in the $J = 1$ than the $J = 0$ level. At zero field, the allowed $v = 0 \rightarrow 1$ transitions between the pairs of inversion

Park et al.

doublets in the symmetric potential are "bottom-to-top" and "top-to-bottom," as required by the dipole selection rule for transitions between opposite-parity inversion–rotation–vibration states. The $Q(1_1^+)$, $Q(1_1^-)$ pair of transitions are top-to-bottom and bottom-to-top, respectively (Fig. 1B, additional information in *SI Appendix*, section A).

An external field along the direction of the molecular c axis distorts the double-minimum potential by stabilizing one of wells by the dipole–field interaction energy ($u = -\boldsymbol{\mu} \cdot \boldsymbol{F}$) and destabilizing the other well by the same energy. In the field-asymmetrized potential, the wavefunctions become localized in either of the 2 wells via Stark mixing of zero-field eigenstates, and become neither symmetric nor antisymmetric with respect to the barrier maximum. This wavefunction localization has been mathematically illustrated for a 1D double-well potential (15). Significantly, the selection rules change from symmetry-allowed (bottom-to-top and top-to-bottom) full well-"delocalized" transitions at zero field to "localized" transitions in the field-asymmetrized potential. In the high-field limit, transitions that originate from the localized wavefunctions in each well dominate. This results in "bottom-to-bottom" and "top-to-top" transition propensity rules (*SI Appendix*, Fig. S4). The change of the selection rules in a strong electric field can be understood in a semiquantitative way by using near-degenerate perturbation theory (*SI Appendix*, section F).

The peak that emerges at 963 cm^{-1} is the bottom-to-bottom transition in $|K| = 1$, shown as a blue solid arrow in the middle PES diagram in Fig. 1D. The 963-cm^{-1} peak blueshifts as the field strength increases until it merges with the red peak. This is principally attributed to the energy shift of the $|K| = 1$ states in $v = 0$. The energy shift at weak field is larger for the $v = 0$ state than for the $v = 1$ state, because the zero-field inversion splitting is much smaller in $v = 0$ (<1 cm^{-1}) than in $v = 1$ (around 24 cm^{-1}) (*SI Appendix*, section F). The bottom level of $|K| = 1$ in $v = 0$, originally 1_1^- at zero field, shifts downward, while that in $v = 1$ shifts very little. This results in the observed blueshift of the bottom-to-bottom transition. The rate of the blueshift is observed to be 2.6 cm^{-1} per 10^7 V/m (illustrated by *SI Appendix*, Fig. S3), which agrees with the dipole–field interaction energy ($u = -\boldsymbol{\mu} \cdot \boldsymbol{F}$) of about 2.4 cm^{-1} at 10^7 V/m. The bottom-to-top transition, shown as a blue dashed arrow in the middle PES diagram in Fig. 1D, is also expected to be blueshifted as the 1_1^- level shifts downward at stronger field, but this transition becomes unobservably weak due to the change in transition selection rule mentioned above. The $Q(1_1^-)$ peak around 980 cm^{-1}, although only barely observable in the spectra in Fig. 1C, follows this expectation. The blueshift of the $Q(1_1^-)$ peak is observed more clearly in a similar experiment conducted with a very thick film at much weaker field (10^6 V/m) (*SI Appendix*, Fig. S5).

For $K = 0$ states, when the field is absent, the $R(0_0^-)$ transition at 975 cm^{-1} is prominent, with a barely noticeable $P(1_0^+)$ transition ([$v = 0$, $J = 1$, $K = 0$, +] → [$v = 1$, $J = 0$, $K = 0$, −]) at 961.5 cm^{-1}. Differently from $|K| = 1$ states, the nuclear permutation symmetry for NH_3 rigorously forbids the existence of 1 member of each inversion doublet (0_0^+, 1_0^-, etc.) in $K = 0$ states (*SI Appendix*, section A).

The $R(0_0^-)$ transition exhibits the following field-dependent behavior: 1) redshift (peak position 975 cm^{-1} at zero field → 972 cm^{-1} at 1.3×10^7 V/m); 2) gradual monotonic increase of intensity; 3) narrowing width (the 2.5-cm^{-1} full width at half maximum at zero field decreases to 1 cm^{-1} at 1.3×10^7 V/m). The gradual increase of intensity and the narrowing of line width indicate that this formerly rotation–vibration transition evolves into a vibrational band origin transition (6, 12) as a result of Stark mixing of the 0_0^- and 1_0^+ states in $v = 1$. In contrast to those in $v = 0$, the 0_0^- and 1_0^+ states in $v = 1$ are reversed in energy order and located close to each other (0_0^- being about 4 cm^{-1} higher in energy than 1_0^+, shown in Fig. 1B). This near-degeneracy of $v = 1$ rotational levels makes them uniquely susceptible to field-induced mixing. Note that the 0_0^- and 1_0^+ states

have the proper symmetries for a Stark-effect interaction. This interaction shifts the lower-lying 1_0^+ state in $v = 1$ downward as the field increases, even faster than that of the 0_0^- state in $v = 0$, resulting in the redshift observed in the Stark spectrum. In addition, the wavefunction mixing transfers some 0_0^- character into the nominal 1_0^+ state. This is the reason that this rotation–vibration transition behaves more like a vibrational band origin transition.

The 2 transitions that evolve in frequency and become prominent in the field region 1.3×10^7 V/m through 3.8×10^7 V/m, one in $|K| = 1$ and the other in $K = 0$, correspond effectively to vibrational band origin transitions. In the strong-field extreme, when the molecular c axis becomes nearly parallel to the field direction and the potential is highly asymmetric, both transitions are localized in the lower well of the asymmetric double-minimum potential. The strong electric field causes the ammonia molecules to librate (rather than rotate) in the harmonic potential well of electrostatic dipole–field interaction. The zero-field 0_0^- and 1_1^- rotational states become correlated at high field with the lowest-lying harmonic librator states (13, 14) (*SI Appendix*, Fig. S6). Because these pairs of harmonic librator states are degenerate in energy, in both $v = 0$ and 1, the 2 transitions merge into a single peak at strong field.

We conduct similar experiments on deuterated ammonia molecules (NH_2D, NHD_2, and ND_3) to make qualitative observations of the isotope effects on the field-driven spectral changes. We expect (1) deuterium substitution to reduce both the inversion tunneling rate and the magnitude of the inversion splitting. Fig. 2 shows the Stark spectra of ammonia isotopologues in the field region of 1×10^7 V/m through 4×10^7 V/m. The coalescing behavior of the 2 peaks is well resolved in the spectra of NH_3 and NH_2D, whereas the evolution of the peaks could only be deduced from changes of the band shape and -width for NHD_2 and ND_3 because the peak separation was narrower than the inherent spectral resolution. NH_2D showed a smaller energy separation and a lower-field coalescence of the peak pairs compared to NH_3 (*SI Appendix*, Fig. S3). In the case of ND_3, top-to-bottom and bottom-to-top transitions in $|K| = 1$, which are $Q(1_1^+)$ and $Q(1_1^-)$ transitions, appeared predominantly at zero field at 760 and 762 cm^{-1}, respectively (*SI Appendix*, section A) (1). As the field increases, these transitions become forbidden and the intensity of the bottom-to-bottom transition increases. The situation is equivalent to the case of $|K| = 1$ states in NH_3; however, the energy splitting of the inversion doublets at zero field is much smaller for ND_3 so that the signature of the spectral evolution induced by electrostatic fields is not clearly resolved. The energy levels and transition selection rules that govern the Stark response would be different for NH_2D and NHD_2 since they are asymmetric-top rotors, unlike NH_3 and ND_3. Detailed analysis will not be discussed
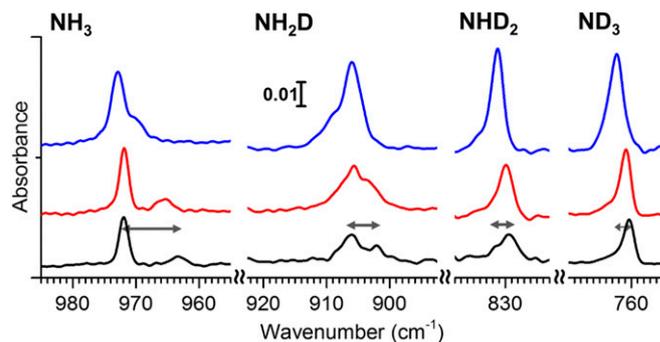

Fig. 2. The Stark spectra of the ν_2 vibrational mode of matrix-isolated ammonia isotopologues. The (black, red, blue) spectra were recorded under external fields at strengths of (1.3, 2.1, 3.6), (1.0, 1.9, 3.4), (1.0, 1.9, 3.4), and (1.3, 2.1, 3.5) $\times 10^7$ V/m for NH_3, NH_2D, NHD_2, and ND_3, respectively. The peak separations are marked by the double-headed arrows.

here. Nevertheless, the isotopologue dependence of the energy separation between transitions, which is marked by horizontal double-headed arrows in Fig. 2, follows the expected decreasing trend of inversion splitting with increased deuteration (24, 12, 6, and 2 cm^{-1} for NH$_3$, NH$_2$D, NHD$_2$, and ND$_3$, respectively) (1). These isotope effects confirm the field-induced asymmetrization of the PES and the corresponding modification of inversion states.

Conclusions

In summary, a very strong DC electric field reversibly orients ammonia molecules in an Ar matrix along the laboratory frame electric-field direction. Infrared Stark spectroscopy of spatially oriented ammonia molecules reveals how the external field modifies the PES for the ν_2 umbrella vibration and produces a sequence of changes in the ν_2 mode transition frequencies and intensities. A noteworthy feature is that Stark-effect vibrational spectroscopy reveals detailed information about the large-amplitude inter- and intramolecular dynamics encoded in static spectra recorded at systematically scanned electric-field strengths. The emergence of vibrational band origin transitions in both $K = 0$ and $|K| = 1$ states and the evolution of these transitions as the field increases from 1.3×10^7 V/m to 3.8×10^7 V/m reveal progressive localization of the wavefunctions as the double-minimum potential becomes increasingly asymmetrized. This corresponds to a change of the inversion dynamics from efficient resonant tunneling to inefficient quenched tunneling. The merging of 2 transitions and a linear blueshift of the coalesced peak at field strength above 4.7×10^7 V/m indicate strong field orientation of no-longer-fluxional ammonia molecules that librate within the deeper minimum of the asymmetric dipole–field interaction potential. We emphasize the existence of a close resemblance between these Stark behaviors of ammonia inversion and those of intramolecular proton transfer in the double-minimum potential observed for tropolone (16) and of tunneling motion of hydrogen fluoride dimer (17) in the gas phase at moderate (10^6 V/m) applied electric-field strengths. The present findings for inversion dynamics of ammonia can help to understand the effects of electric fields on analogous tunneling phenomena in more complex molecules. This work demonstrates that, with the help of a continuously tuned strong DC electric field, frequency-domain spectroscopy can give information about the changes of molecular eigenstate energies and wavefunctions that develop due to the field-induced change of the PES. This class of DC spectroscopy gives important insights into dynamics. The accuracy and multifeature nature of these frequency-domain spectra offer advantages over time-resolved ultrafast measurements, which monitor the evolution of multiple wavepackets induced by ultrashort laser pulses interacting with nonoriented molecules. The infrared Stark-effect spectrum of ammonia provides a "user's guide" to how molecules are affected by a strong DC external electric field, which can be present in diverse chemical environments.

Materials and Methods

The experiments were performed in an ultrahigh vacuum chamber, the detailed description of which can be found elsewhere (11, 18, 19). The molecular film was prepared on a Pt(111) substrate surface maintained at a cryogenic temperature (about 10 K) by sequential deposition of corresponding gases.

D$_2$O (Aldrich, 99 at. % D) was purified by freeze–pump–thaw cycles. Ar and NH$_3$ gases were used directly from commercially available gas cylinders. ND$_3$ was prepared by thermal evaporation of ND$_3$ molecules from ND$_4$OD solution (Alfa Aesar, 99 at. % D, 23.0 to 27.0 wt. % sol), utilizing the large vapor pressure of ammonia relative to that of water. NH$_2$D and NHD$_2$ were prepared similarly, from a roughly 1:1 mixture of NH$_4$OH solution (Samchun Chemical Co., Ltd., Korea, 28.0 to 30.0 wt. % sol) and liquid D$_2$O to give an isotopologue distribution of NH$_3$:NH$_2$D:NHD$_2$:ND$_3$ = 1:3:3:1.

A thin film sample of matrix-isolated ammonia was prepared by code-position of ammonia and Ar gases with a predetermined NH$_3$:Ar partial-pressure ratio on the order of 10^{-3} (11, 19). The sample had a stacked structure of an Ar film (144 to 960-ML thickness; ML = monolayer; 1 ML = 1.1×10^{15} molecules per cm^{-2}) that contained ammonia molecules, sandwiched between 2 Ar spacer layers (48 to 120 ML each). The spacer layers prevent the ammonia molecules from being affected by interfacial effects. The upper Ar film was capped by an amorphous D$_2$O film (25 ML). The thickness of the entire sample was 150 to 710 nm. A schematic drawing of the sample is shown in Fig. 1A.

A static electric field was generated across the film using the previously demonstrated (9, 11) ice film nanocapacitor method. The field strength was increased by soft-landing Cs$^+$ ions on the capping D$_2$O film surface (Fig. 1A) and decreased by spraying low-energy (~3 eV) electrons onto the Cs$^+$-deposited film surface. The strength of the externally applied electric field within the Ar matrix was estimated from the film voltage measured with a Kelvin probe. All measured values of field strength given in this paper are the macroscopic field (F_0), estimated simply by dividing the voltage across the film by the thickness of the film. The actual field strength (F) that a matrix-isolated molecule experiences is expressed by $F = c_{local}F_0$, where the local field correction factor, c_{local}, is estimated to be in the range of $1 \sim 2$ (11) by assuming that an ammonia molecule is located inside a cavity in the dielectric continuum of the matrix and using classical electrostatics and Onsager reaction-field theory (20, 21).

RAIRS measurements were conducted with a Fourier transform infrared spectrometer with a liquid nitrogen-cooled mercury-cadmium telluride detector in grazing angle reflection geometry (85°) (19). An incident infrared beam was p-polarized by a wire grid polarizer. The RAIR spectra were averaged 256 times at a spectral resolution of 1 cm^{-1}.

1. L. Abouaf-Marguin, M. E. Jacox, D. E. Milligan, The rotation and inversion of normal and deuterated ammonia in inert matrices. *J. Mol. Spectrosc.* **67**, 34–61 (1977).
2. M. Behrens *et al.*, Rotationally resolved IR spectroscopy of ammonia trapped in cold helium clusters. *J. Chem. Phys.* **109**, 5914–5920 (1998).
3. M. E. Jacox, W. E. Thompson, The infrared spectrum of NH$_3$-d_n trapped in solid neon. *J. Mol. Spectrosc.* **228**, 414–431 (2004).
4. M. N. Slipchenko, A. F. Vilesov, Spectra of NH$_3$ in He droplets in the 3 μm range. *Chem. Phys. Lett.* **412**, 176–183 (2005).
5. M. Ruzi, D. T. Anderson, Matrix isolation spectroscopy and nuclear spin conversion of NH$_3$ and ND$_3$ in solid parahydrogen. *J. Phys. Chem. A* **117**, 9712–9724 (2013).
6. J. M. Rost, J. C. Griffin, B. Friedrich, D. R. Herschbach, Pendular states and spectra of oriented linear molecules. *Phys. Rev. Lett.* **68**, 1299–1302 (1992).
7. M. Y. Choi *et al.*, Infrared spectroscopy of helium nanodroplets: Novel methods for physics and chemistry. *Int. Rev. Phys. Chem.* **25**, 15–75 (2006).
8. S. G. Boxer, Stark realities. *J. Phys. Chem. B* **113**, 2972–2983 (2009).
9. S. Shin *et al.*, Generation of strong electric fields in an ice film capacitor. *J. Chem. Phys.* **139**, 074201 (2013).
10. S. Süzer, L. Andrews, FTIR spectra of ammonia clusters in noble gas matrices. *J. Chem. Phys.* **87**, 5131–5140 (1987).
11. Y. Park, H. Kang, H. Kang, Brute force orientation of matrix-isolated molecules: Reversible reorientation of formaldehyde in an argon matrix toward perfect alignment. *Angew. Chem. Int. Ed. Engl.* **56**, 1046–1049 (2017).
12. H. Kang, Y. Park, Z. H. Kim, H. Kang, Electric field effect on condensed-phase molecular systems. VI. Field-driven orientation of hydrogen chloride in an argon matrix. *J. Phys. Chem. A* **122**, 2871–2876 (2018).
13. M. Härtelt, B. Friedrich, Directional states of symmetric-top molecules produced by combined static and radiative electric fields. *J. Chem. Phys.* **128**, 224313 (2008).
14. A. Maergoiz, J. Troe, Weak- and strong-field Stark energy levels of symmetric top dipolar molecules. *J. Chem. Phys.* **99**, 3218–3223 (1993).
15. B. Burrows, M. Cohen, T. Feldmann, Localization effects in a double-well model. *Can. J. Phys.* **76**, 129–142 (1998).
16. C. Wu, Y. He, W. Kong, Polarization spectroscopy of gaseous tropolone in a strong electric field. *J. Chem. Phys.* **121**, 4577–4584 (2004).
17. R. J. Bemish, M. C. Chan, R. E. Miller, Molecular control using dc electric fields: Quenching of the tunneling in HF dimer. *Chem. Phys. Lett.* **251**, 182–188 (1996).
18. H. Kang, S. Shin, Y. Park, H. Kang, Electric field effect on condensed-phase molecular systems. III. The origin of the field-induced change in the vibrational frequency of adsorbed CO on Pt (111). *J. Phys. Chem. C* **120**, 17579–17587 (2016).
19. Y. Park, J. H. Lim, J. Y. Lee, H. Kang, Electric field effect on condensed-phase molecular systems. VII. Vibrational Stark sensitivity of spatially oriented water molecules in an argon matrix. *J. Phys. Chem. C* **123**, 9868–9874 (2019).
20. C. J. F. Böttcher, *Theory of Electric Polarization* (Elsevier, Amsterdam, ed. 2, 1973).
21. L. Onsager, Electric moments of molecules in liquids. *J. Am. Chem. Soc.* **58**, 1486–1498 (1936).

CHEMISTRY